Hydrological Sciences Journal

ISSN: (Print) (Online) Journal homepage: https://www.tandfonline.com/loi/thsj20

Modelling daily streamflow in a temporary karst river system: comparing three approaches using the SWAT model

Giovanni Francesco Ricci, Marco Centanni, Anna Maria DeGirolamo & Francesco Gentile

To cite this article: Giovanni Francesco Ricci, Marco Centanni, Anna Maria DeGirolamo & Francesco Gentile (2023): Modelling daily streamflow in a temporary karst river system: comparing three approaches using the SWAT model, Hydrological Sciences Journal, DOI: 10.1080/02626667.2023.2174027

To link to this article: https://doi.org/10.1080/02626667.2023.2174027

Published online: 21 Feb 2023.

HYDROLOGICAL SCIENCES JOURNAL
https://doi.org/10.1080/02626667.2023.2174027

Modelling daily streamflow in a temporary karst river system: comparing three approaches using the SWAT model

Giovanni Francesco Ricci [a], Marco Centanni [a], Anna Maria DeGirolamo [b] and Francesco Gentile [a]

[a]Department of Agricultural and Environmental Sciences, University of Bari Aldo Moro, Bari, Italy; [b]Water Research Institute (IRSA-CNR), National Research Council, Bari, Italy

ABSTRACT

This work tests different options for simulating hydrology in basins with karst areas. The Soil and Water Assessment Tool (SWAT) model was applied to the Canale d'Aiedda (Puglia, Italy), a Mediterranean temporary karst river basin. Different basin delineations and model parameterizations were adopted that include: (i) cutoff of the karst areas (configuration A); (ii) basin set-up including the karst areas (configuration B) and (iii) model parameterization considering a bypass flow in karst sub-basins (configuration C). The model performance was satisfactory for daily streamflow for configurations B and C and good for A. A better simulated large floods. C presented the best fit for monthly streamflow from May to July. Regarding the water balance, C showed higher values of surface runoff and lower values of total water yield than A and B. Bypass flow proved to be a valid option to improve the simulation of the hydrological processes in karst areas.

ARTICLE HISTORY
Received 25 July 2022
Accepted 20 December 2022

EDITOR
A. Fiori

ASSOCIATE EDITOR
G. Jeelani

KEYWORDS
SWAT model; karst areas; Mediterranean basin; hydrological regime; crack flow function

1 Introduction

The flow intermittency in a river is influenced by several factors such as lithology, geomorphology, rainfall, and temperature (Fortesa *et al.* 2021, Sauquet *et al.* 2021). In particular, the presence of karst (limestone), can increase the formation of geomorphological features (e.g. caves, dolines, sinkholes) that lead to an increase in the intermittency of the streams (Jakada and Chen 2020, Fovet *et al.* 2021). Karst areas, as well as temporary rivers, are very common in the Mediterranean region (Sauquet *et al.* 2021). Malagò *et al.* (2016) point out that carbonate rocks cover about 35% of the European territories and that limestones are very thick and shallow in some areas of Spain, southern France, the Balkan Peninsula, Turkey, and Italy. In all of these countries, temporary rivers are predominant and constitute an important source for both human activities and ecological features (Poff *et al.* 1997, Acuña *et al.* 2014, Oueslati *et al.* 2015, Datry *et al.* 2017).

Like perennial rivers, temporary rivers are also fundamental to the achievement of the "good ecological status" specified in the European Commission (EC) Water Framework Directive (EC 2000) and promoted in the Green Deal's (GD) Farm to Fork strategy and Zero Pollution action plan (EC 2019). However, for a long time, environmental policies have been focused mainly on perennial rivers, and temporary rivers have often been less investigated and monitored (Nikolaidis *et al.* 2013b, Soria *et al.* 2021). The lower interest in temporary rivers leads to less investment in terms of monetary resources, which are necessary for monitoring plans (i.e. installing and maintaining gauging stations) and managing the river ecosystems. Monitoring is limited also because most of the instruments are unable to correctly measure values of flow close to zero (Tramblay *et al.* 2020, van Meerveld *et al.* 2020). Hence, flow time series are often unavailable or incomplete in temporary river systems, making hydrological studies challenging (D'Ambrosio *et al.* 2017, Borg Galea *et al.* 2019).

Models may be used to generate long time series of streamflow data to be used to classify and characterize the flow regime of these rivers (Meresa 2019, Fortesa *et al.* 2021). These models, however, require a lot of input data and an in-depth knowledge of basin-scale hydrological processes (Eini *et al.* 2020, Ricci *et al.* 2020). The complexity of karst areas, in terms of fast groundwater flows, springs, sinkholes, and dolines, represents a challenge for modelling activities (Amin *et al.* 2017, Martínez-Salvador and Conesa-García 2020).

The Soil and Water Assessment Tool (SWAT; Arnold *et al.* 1998) is one of the most widely used hydrological models in different geographical areas (Borrelli *et al.* 2016, Amin *et al.* 2017). A large number of modelling applications make it possible to highlight the critical points that need particular attention when simulating hydrological processes. Specifically, in basins with intermittent rivers, the extremely low flow and the dry conditions are critical points in the streamflow predictions (De Girolamo *et al.* 2017); the water exchanges from river and groundwater systems are still predicted with low accuracy (Jimeno-Sáez *et al.* 2018, Senent-Aparicio *et al.* 2020, Sánchez-Gómez *et al.* 2022). These criticisms are accentuated in Mediterranean basins and in karst areas where the presence of specific karst features (e.g. caves, dolines, sinkholes) dramatically influence some hydrological processes such as infiltration (Eini *et al.* 2020). Research and applications are needed to improve the modelling predictions in these environments (De Girolamo *et al.* 2022a).

CONTACT Giovanni Francesco Ricci giovanni.ricci@uniba.it Department of Agricultural and Environmental Sciences, University of Bari Aldo Moro, Via Amendola 165/A, 70126 Bari, Italy

The number of studies related to karst areas is still limited, although some modelling approaches have been tested (Jakada and Chen 2020). As evidenced in the review by Eini *et al.* (2020), some authors coupled SWAT with another model, and some modified the model algorithm, while others focused their study on model parameterization. Nikolaidis *et al.* (2013a) and Nerantzaki *et al.* (2015) used two karst models coupled with SWAT to improve the simulation of spring discharge and to account for the change in the flow recession phase. Baffaut and Benson (2009) improved the computation of the deep groundwater recharge in order to simulate the effect of the sinkholes in their SWAT-B&B (SWAT-Baffaut and Benson). Malagò *et al.* (2016) integrated the two previous approaches in their KSWAT (karst-flow model-SWAT) to better represent the higher hydraulic conductivity up to the deep aquifer and the faster movement of water through the subsurface. Vale and Holman (2009) and Martínez-Salvador and Conesa-García (2020), in contrast, calibrated SWAT by focusing on infiltration/runoff and groundwater processes. The results of these model applications are often contradictory. Indeed, the performances vary from unsatisfactory to good. Most of the studies that report good results are calibrated on a monthly scale, while those calibrated on a daily scale – half of the studies investigated – showed often satisfactory or poor performances (Eini *et al.* 2020). Moreover, some model code modifications are not available for further public use (Jakada and Chen 2020), thus replicating these approaches would require specific programming skills and cannot be carried out easily by most users. Hence, there is a need to further investigate modelling approaches to be applied in karst areas.

The general aim of the present work was to identify the most suitable approach to simulate the daily streamflow of a temporary river system in a karst area, comparing different reliable procedures that do not require SWAT model code modifications. To do this, a case study was analysed where different modelling approaches were adopted with the following specific aims: (i) simulate daily streamflow in a temporary river system including karst areas in the river basin schematization; (ii) simulate daily streamflow excluding karst areas in the river basin schematization; and (iii) simulate daily streamflow including in the calibration process the "crack flow function." Specifically, the SWAT model was implemented in the Canale d'Aiedda basin (SE Italy), which is characterized by karst formations in its mountainous areas. The results will allow modellers to select the most appropriate modelling approach for simulating streamflow in river basins with karst areas.

2 Materials and methods

2.1 Study area

The Canale d'Aiedda basin is located in Southern Italy within the territory of the province of Taranto (Apulia Region) and flows into the Mar Piccolo (Fig. 1). The total drainage area is 360 km^2, the average altitude is 168 m a.s.l., ranging from 0 m to 517 m, and the mean slope is 2.7° (D'Ambrosio *et al.* 2019).

The climate is characterized by a mean annual rainfall and temperature (2000–2013) ranging from 601 to 865 mm and from 8.1°C (January) to 27.9°C (August), respectively. In summer and autumn, rainfalls generally are characterized by high intensity and short duration events. Agriculture is the main anthropogenic activity in the basin. Vineyards, olive trees, almond trees, orange groves, vegetables, and arable land are the main land uses and cover almost 88% of the total area. Natural areas, which extend for 6% of the basin surface, are characterized by deciduous and coniferous forests, pastures, brushes, and shrubs. Urban areas are of medium size and occupy 4% of the total basin area (D'Ambrosio *et al.* 2020). Soils range from clayey silt to sandy loam. Three wastewater treatment plants (WWTPs), located in the municipalities of Montemesola, Monteiasi, and San Giorgio Ionico (Fig. 1), flow into the river system, which is mainly characterized by concrete beds and banks.

Arenitic units in the central part of the basin and fractured limestone carbonate rocks in the northeastern part (De Girolamo *et al.* 2019) are the main geological units. The karst structure is characterized by a high water infiltration rate, which leads to deep groundwater recharge since the shallow aquifer is narrow and discontinuous (De Filippis *et al.* 2017). The deep aquifer feeds several submarine springs, called "citri" (Polemio *et al.* 2008, Lisco *et al.* 2016). Due to this particular hydrogeological structure, the groundwater flow in this area can be much higher than the surface discharge (Zuffianò *et al.* 2016).

The flow regime in the upstream parts is in near-natural conditions and it shows an intermittent character. In the lowlands, the flow regime is altered and it is mostly permanent due to WWTP discharges. The main course flows into a protected area called "Palude la Vela Regional Nature Reserve," which is part of the Site of Community Importance (SIC) "Mar Piccolo" (IT9130004). This wetland is an important environmental area for its ecological biodiversity, especially considering the birdlife and the plant species typical of the Mediterranean maquis (D'Ambrosio *et al.* 2020).

2.2 SWAT model

SWAT is one of the most commonly used hydrological and water quality models. It is a semi-physical spatially distributed model used to predict streamflow, sediment, and nutrient loads in gauged and ungauged river basins (Arnold *et al.* 1998, Borrelli *et al.* 2021). SWAT was developed in the 1990s by the United States Department of Agriculture – Agricultural Research Service (USDA-ARS) (Arnold *et al.* 2012a). The model divides the area of a basin into sub-basins through a threshold defined by the user that identifies the minimum drainage area necessary to delineate the watercourse. Furthermore, SWAT divides the sub-basins into hydrological response units (HRUs), which are the basic unit for the water balance calculations, based on defined thresholds referring to land use, slope, and soil properties (Neitsch *et al.* 2011). Surface runoff may be computed by choosing the Soil Conservation Service curve number method (SCS-CN, 1972) or the Green-Ampt infiltration method (Green and Ampt 1911). The potential evapotranspiration (PET) can be estimated by the Penman-Monteith (Monteith 1965), the Priestly-Taylor (Priestley and Taylor 1972), and the Hargreaves

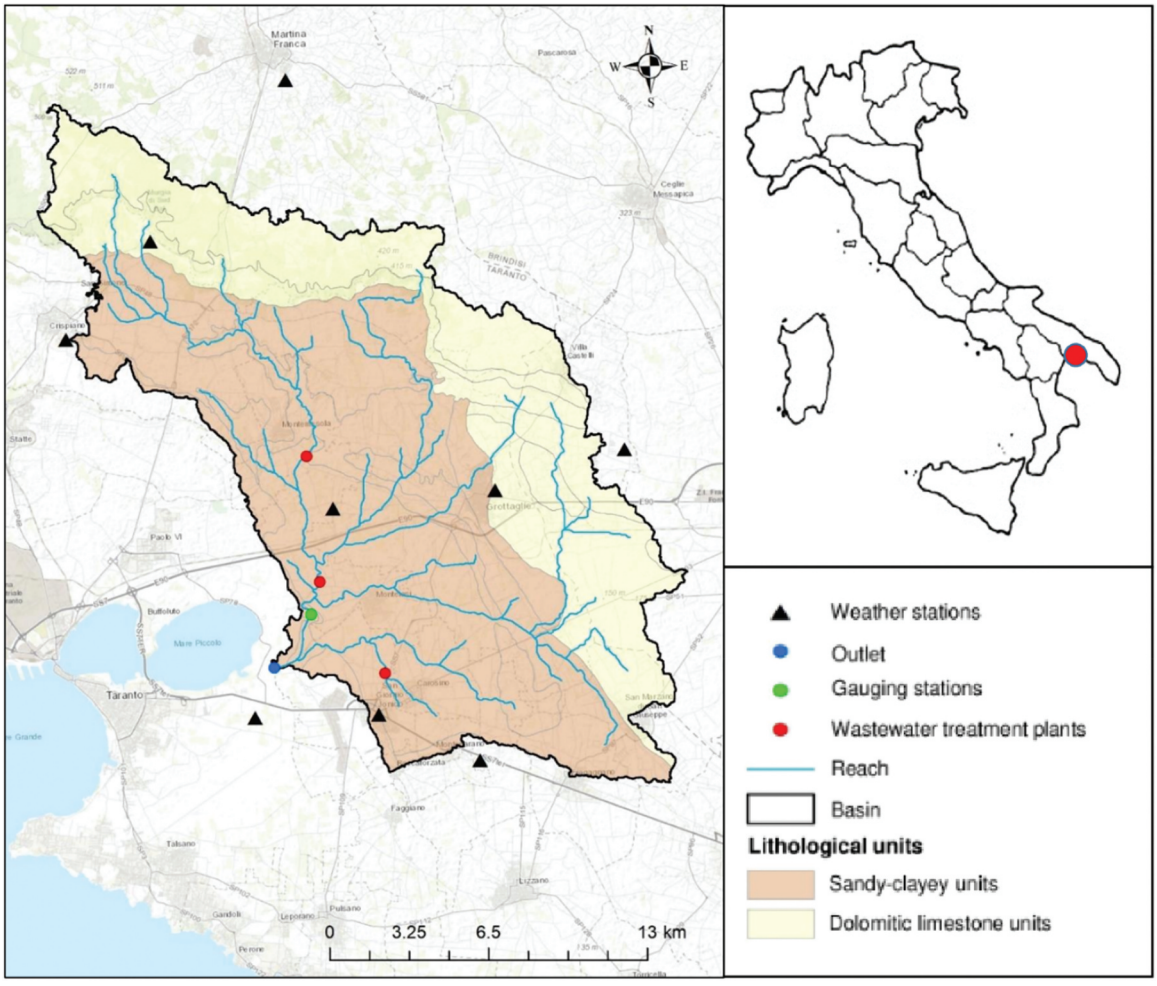

Figure 1. Study area: the Canale d'Aiedda Basin, Apulia Region (SE, Italy).

methods (Hargreaves and Samani 1985). In this work, the Hargreaves method was used to calculate PET, while the SCS-CN method was used for the surface runoff.

2.2.1 Conceptual model

SWAT 2015 was used in this study (Winchell *et al.* 2013). The input data required by the model, and used for the model set-up, are provided in Table 1. In the Canale d'Aiedda basin and the surrounding area, nine weather stations were available (Fig. 1). The meteorological data were available from 1997 to 2019 on a daily time scale. However, solar radiation, wind speed, and relative humidity time series presented a lot of gaps. Hence, the Hargreaves method was preferred to estimate potential evapotranspiration since it requires only daily temperature data. Mean annual volumes of treated wastewater were available for the three WWTPs (1997–2019). The land use and soil data were properly processed and included in the SWAT geodatabase. Twenty-one classes for land use and 11 for soil type were found in the study area (D'Ambrosio *et al.* 2019). The management practices of the main crops were collected through farmers' interviews and included in the model set-up. For the vineyard, two shallow (10 cm) and one deep (35 cm) tillage operations were adopted in February, May, and October, respectively. Fertilizers were applied in

Table 1. Source and spatial resolution of the input data used for the SWAT model set-up.

Input	Source	Resolution
Digital terrain model	Puglia Region (http://www.sit.puglia.it)	8 × 8 m
Land use map	Puglia Region (http://www.sit.puglia.it)	1:5000
	National Agricultural Census (http://censimentoagricoltura.istat.it/index.php?id=73)	–
Soil map and database	Puglia Region (2001)	1:100 000
	Joint Research Centre European Soil Data Centre (JRC-ESDAC) (https://esdac.jrc.ec.europa.eu/resource-type/datasets)	500 × 500 m
Point sources	Apulian Water Authority (personal communication)	–
	Regional Agency for Environmental Protection (http://www.arpa.puglia.it/web/guest/depuratori)	
	Puglia Region (http://www.sit.puglia.it)	
Meteorological data	Civil Protection Service – Puglia Region (https://protezionecivile.puglia.it/)	–
	Regional Agency for Irrigation and Forestry Activities (http://www.agrometeopuglia.it/)	
Agricultural practices	Interviews with farmers and agricultural advisors (D'Ambrosio *et al.* 2019)	–

February (type 12-12-17[1] and 10-5-15[1]) in October and in November (organic manure for both). The irrigation season started in May and ended in September, with a total amount of applied water of 2400 $m^3ha^{-1}year^{-1}$. For olives, three shallow tillage operations were adopted, in April, August, and November. Fertilizers were applied in April (urea and 12-8-8[1]) and in August (13-46-00[1]), while irrigation was included in the management operations from June to September with a total amount of applied water of 500 $m^3ha^{-1}year^{-1}$. Durum wheat was the major crop (planting was set in November and harvesting in July), for which deep and shallow tillage operations were carried out in August and October, respectively, and fertilizers were applied in December (25–15–00[1]) and in February (urea). Finally, for the minor crops (e.g. minor orchards) two tillage operations were set in spring (shallow) and autumn (deep), respectively. The functions of auto-irrigation and auto-fertilization were used. The USLE P (Universal Soil Loss Equation - Support practice factor) factor was set to 1 because of the lack of conservative practices adopted in the study area.

2.2.2 River basin schematization

Three configurations, based both on a diverse GIS (Geographic information system) schematization of the basin and sub-basins and on different calibration approaches, were tested in this work. In the first configuration (configuration A, Fig. 2), the karst areas, located on the northern and eastern edges of the basin, were cut off from the basin delineation since these were considered not effectively contributing to surface runoff (D'Ambrosio *et al.* 2020). The absence of streamflow within the river network in this karst area was confirmed also by field surveys carried out at different periods of the year (Ricci *et al.* 2022a). With this approach, the drainage area was 222 km^2. In the second approach (configuration B, Fig. 2), the karst areas were included in the basin delineation, which resulted in an area of 360 km^2. In the third approach (configuration C), the whole basin (including karst areas) was calibrated by activating the "crack flow function" (ICRK; basin.bsn file). This bypass flow module was introduced by Arnold *et al.* (2005) to replicate the formation of the cracks in Vertisols. The volume of cracks increases in the dry period and the amount of water infiltrating into soils during rainfall events is equal to the volume of the cracks (Neitsch *et al.* 2011). For this reason, this function has also been applied to represent the increment of infiltration due to karst geomorphological features (Jarvis *et al.* 2016, Kan *et al.* 2019, Eini *et al.* 2020). In configuration C, to provide the most accurate

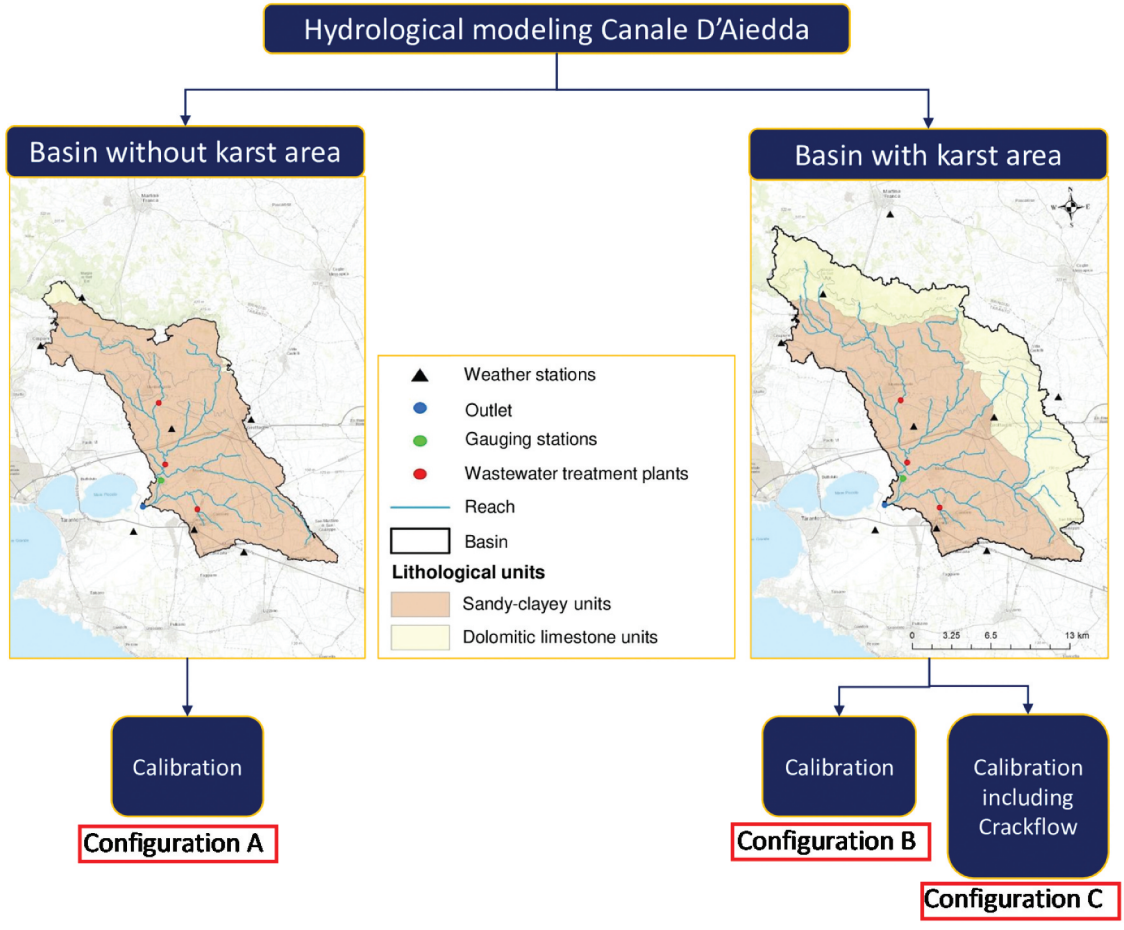

Figure 2. Scheme of the three different approaches adopted for the SWAT model configuration of the Canale D'Aiedda.

[1]The order of the numbers refers to the chemical substances of which the fertilizer is made (i.e. N-P_2O_5-K_2O).

simulation of the karst areas, the Sol_CRK parameter was calibrated only in the HRUs corresponding to outcropping limestone (Fig. 2).

After fixing the minimum drainage area of each sub-basin (350 ha), the river basin was sub-divided into 40 sub-basins (Fig. 3(a, c)) in configuration A, and 68 sub-basins in configurations B and C (Fig. 3(b, d)). Moreover, to discretize HRUs, thresholds of 10%, 10%, and 20% for land use, soil properties, and slopes, respectively, were set, generating 271 HRUs in configuration A and 480 in configurations B and C. Before proceeding with the calibration of the model it was verified that the threshold used ensured the original proportion of land use and soil type and that only minor classes of land use or soils were not considered.

SWAT was run from 1997 to 2019, at a daily time scale, including a warm-up period of three years, for all the three configurations. The model, which uses the centroid method to assign a wheatear station to a specific sub-basin (Neitsch *et al.* 2011), selected seven stations in configuration A and nine in configuration B and C (Fig. 2).

2.2.3 Model calibration

The calibration was then performed by means of the SWAT-CUP (SWAT-Calibration and Uncertainty Programs) tool using the Sequential Uncertainty Fitting (SUFI-2) algorithm (Abbaspour 2015) and setting an objective function for the Nash-Sutcliffe efficiency (NSE; Nash and Sutcliffe 1970) higher than 0.5. The same tool was also used to perform the sensitivity analysis (D'Ambrosio *et al.* 2020). An initial range of parameters was selected based on the knowledge of the processes occurring in the basins (Arnold *et al.* 2015). The monitoring of streamflow at the gauging station (Fig. 1) covered the period from August 2017 to December 2019 on a daily scale. To obtain a more robust set of calibrated parameters, and to better represent all the hydrological conditions (dry and wet

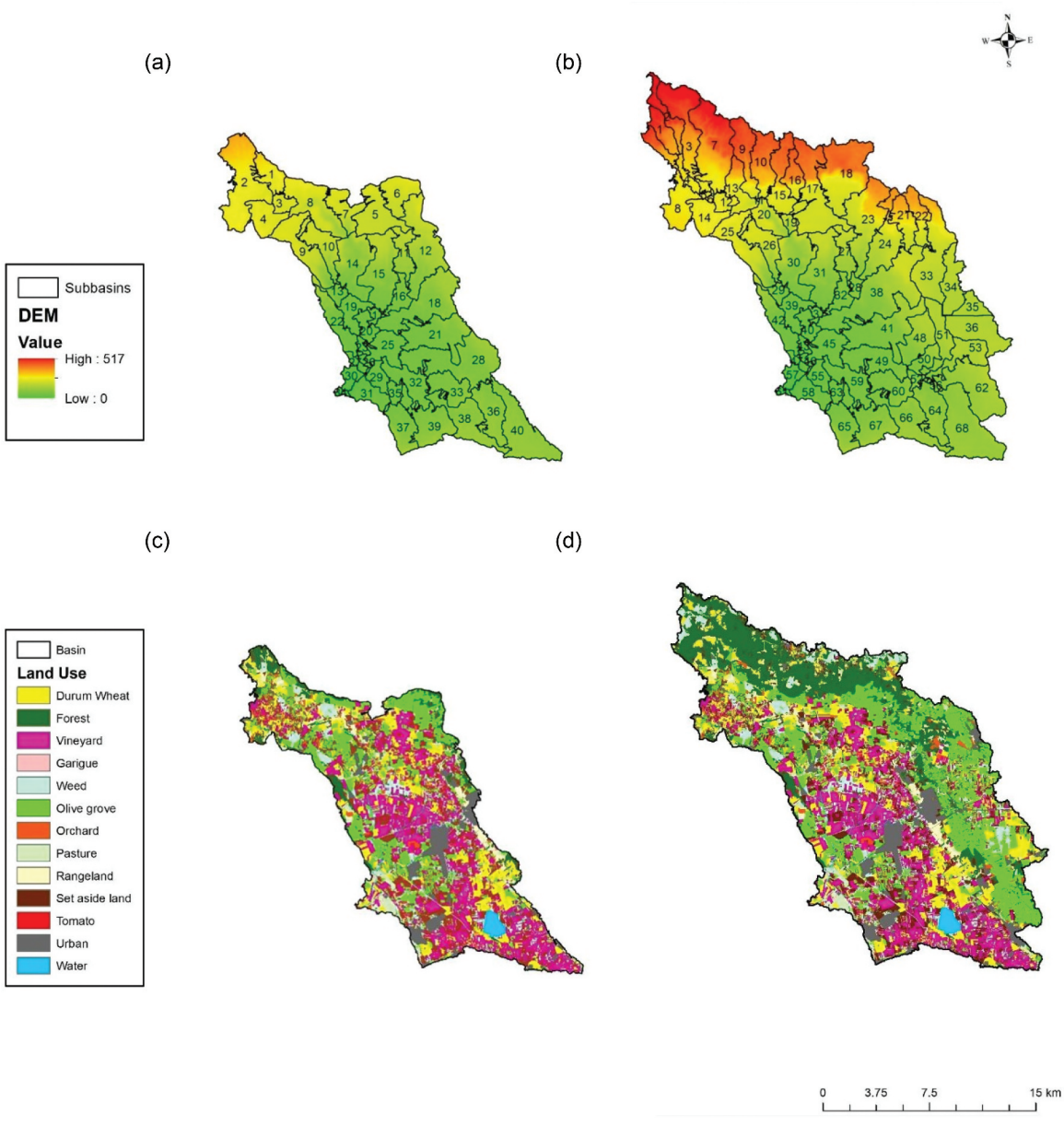

Figure 3. SWAT basin schematizations: (a) digital elevation models (DEMs) and sub-basins for configuration A; (b) DEMs and sub-basins for configuration B and C; (c) land use for configuration A; and (d) land use for configurations B and C.

conditions), the entire dataset of measurements was used for calibrating the model (Arsenault *et al.* 2018, Ricci *et al.* 2022a). For configurations A and B, the model was calibrated working on the same parameters that assumed different values (Table 2). In configuration C, in addition to the parameters selected in configuration B, the crack flow function was activated for those sub-basins that overlapped the karst areas. Model performances were evaluated using the NSE, percent bias (PBIAS), and coefficient of determination (R^2). The model performance was considered satisfactory if NSE and R^2 were higher than 0.5 and if PBIAS fell within the range −25% to +25% (Moriasi *et al.* 2007).

3 Results

3.1 Model calibration

Statistical performances for the calibration at the daily time scale were good for configuration A and satisfactory for B and C (without and with the crack flow function activated, respectively) (Table 3). The SWAT model underestimated the streamflow in configuration A (PBIAS +5.1) and configuration B (PBIAS +25.4), while it overestimated the streamflow in configuration C (PBIAS −2.0).

During the study period, the mean daily streamflow was estimated at 0.043, 0.055, and 0.059 m^3s^{-1} for configurations A, B, and C, respectively. These values matched well with the measured ones (0.058 m^3s^{-1}). Large floods were generally well represented in configuration A (Fig. 4(a)); meanwhile, they were underestimated in configurations B and C (Fig. 4(b) and (c)). In particular, the highest measured peak flow, which occurred on 23 August 2018, was 2.67 m^3s^{-1}, which resulted in overestimation in configuration A (2.85 m^3s^{-1}), and underestimation in configurations B (1.74 m^3s^{-1}) and C (1.78 m^3s^{-1}) (Fig. 4(a–c)). Small floods recorded in winter were generally well predicted by configuration C (Fig. 4(c)).

3.2 Annual and monthly streamflow

The flow duration curves (Fig. 5) show that the best prediction for the extremely high flow (0–4%) was relative to configuration C. The normal flow (4–20% exceedance frequency) was underestimated in the three configurations, but configuration C performed better than A and B since there is a good correspondence between 20% and 30% of exceedance frequency. All the configurations overestimated low flow (30–90%) (Fig. 5) with a comparable pattern; meanwhile, configuration

Table 2. Calibrated parameters, description, and their fitted values for configurations A, B, and C. The letter before the code of the parameter stands for the methodology adopted in SWAT-CUP to apply changes. V corresponds to the replacement of the original value with the new values reported in the row; R corresponds to the multiplication of the original values by 1 + the value reported in the row. Values in bold are the calibrated ranges of values obtained with the R method.

Parameter	Description	Fitted value Configuration A	Fitted value Configuration B	Fitted value Configuration C
V__EVRCH.bsn	Reach evaporation adjustment factor	0.87	0.95	0.87
V__SURLAG.bsn	Surface runoff lag time	11.95	9.10	19.30
V__TRNSRCH.bsn	Fraction of transmission losses from main channel that enter deep aquifer	0.53	0.52	0.55
R__CN2.mgt	SCS runoff curve number	0.21	0.19	0.21
		98–48	**98–69**	**98–69.2**
V__BIOMIX.mgt	Biological mixing efficiency	0.62	0.22	0.98
V__ALPHA_BF.gw	Baseflow alpha factor (days)	0.29	0.36	0.34
V__GW_DELAY.gw	Groundwater delay (days)	42.05	21.35	65.71
V__GWQMN.gw	Threshold depth of water in the shallow aquifer required for return flow to occur (mm)	2222.121	1619.32	3620.73
V__REVAPMN.gw	Threshold depth of water in the shallow aquifer for "revap" to occur (mm)	749.15	387.74	288.77
V__RCHRG_DP.gw	Deep aquifer percolation fraction	0.85	0.50	0.85
V__GW_REVAP.gw	Groundwater "revap" coefficient	0.18	0.06	0.18
R__SOL_K.sol	Saturated hydraulic conductivity	−0.11	−0.44	0.45
		24.82–0.05	**15.52–0.03**	**40.33–0.09**
R__SOL_AWC.sol	Available water capacity of the soil layer	−0.10	0.19	0.27
		0.11–0.07	**0.15–0.09**	**0.17–0.10**
R__SOL_Z.sol	Depth from the soil surface to the bottom of the layer	−0.23	−0.05	−0.05
		1531.77–22.97	**1898.43–28.47**	**1898.43–28.47**
V__EPCO.hru	Plant uptake compensation factor	0.89	0.49	0.73
V__ESCO.hru	Soil evaporation compensation factor	0.68	0.89	0.98
V__CANMX.hru	Maximum canopy storage – vineyard	4.14	32.10	73.33
V__CANMX.hru	Maximum canopy storage – olive groves	5.37	100	68.48
V__CANMX.hru	Maximum canopy storage – durum wheat	0.32	44.64	71.10
V__CANMX.hru	Maximum canopy storage – garigue	2.22	56.07	21.43
V__CANMX.hru	Maximum canopy storage – rangeland	0.07	88.57	85.94
V__CANMX.hru	Maximum canopy storage – pasture	2.33	39.91	59.07
V__CANMX.hru	Maximum canopy storage – mixed forest	3.29	28.68	43.79
V__CANMX.hru	Maximum canopy storage – deciduous forests	4.30	25.58	74.43
V__CH_K1.sub	Effective hydraulic conductivity in tributary channel alluvium	29.67	69.81	39.79
V__CH_N1.sub	Manning's "n" value for the tributary channels	10.07	20.09	14.50
V__CH_K2.rte	Effective hydraulic conductivity in main channel alluvium	43.23	27.46	16.22
V__CH_N2.rte	Manning's "n" value for the main channel	0.28	0.26	0.21
V_SOL_CRK	Crack volume potential of soil	-	-	0.90

Table 3. Statistical performances of the SWAT model calibration at a daily time step. R^2: coefficient of determination; NSE: Nash-Sutcliffe efficiency; PBIAS: percent bias.

Configuration	R^2	NSE	PBIAS
A	0.72	0.71	+5.1
B	0.57	0.56	+25.4
C	0.59	0.59	−2.0

B showed the best performance in the extremely low flow (90–100%).

The results of the different configurations adopted in the present study in terms of mean monthly streamflow are reported in Fig. 6. Configuration B showed values of mean monthly flow lower than A and C, and also lower than the observed streamflow (except for July). During the wet months (from October to January), configuration C showed values of mean monthly streamflow higher than B and A and also higher than measured streamflow. From May to June, C presented the best fit with measured monthly streamflow.

From January to April, configuration A underestimated the measured monthly streamflow, whereas from September to December a good fit was predicted; meanwhile, from May to July streamflow was overestimated.

3.2 Water balance components

The average annual components of the water balance for the three configurations are reported in Table 4 (2017–2019). The potential evapotranspiration (Eto) is about double that of rain (Pcp) ranging from 1161.6 mm to 1191.7 mm. Due to the different rainfall stations considered in the three basin schematizations, Pcp was about 621.4 mm for configuration A and 644.7 for B and C.

Actual evapotranspiration was estimated at 569.8 and 575.9 mm, for A and B, respectively, and 534.4 mm for configuration C. Surface runoff was about 73.5 mm (11.8% of Pcp) in configuration A, about 51.6 mm (8% of Pcp) in B and 18.8 mm (3% of Pcp) for C. Total flow (average annual flow out of the reach at the gauging station, mm) was well predicted by the three configurations (5.5, 4.3, and 5.9 mm in configurations A, B, and C, respectively) since the values were very close to the measured ones (5.80 mm). Total water yield (TWY, total flow + deep aquifer recharge − transmission losses) assumed different values: in configuration A it was about 136.5 mm (22% of Pcp), in B it was 96.2 mm (about 15% of Pcp), and it was about 142.3 mm (22% of Pcp) in C. It is important to underline that TWY in A and C constituted the

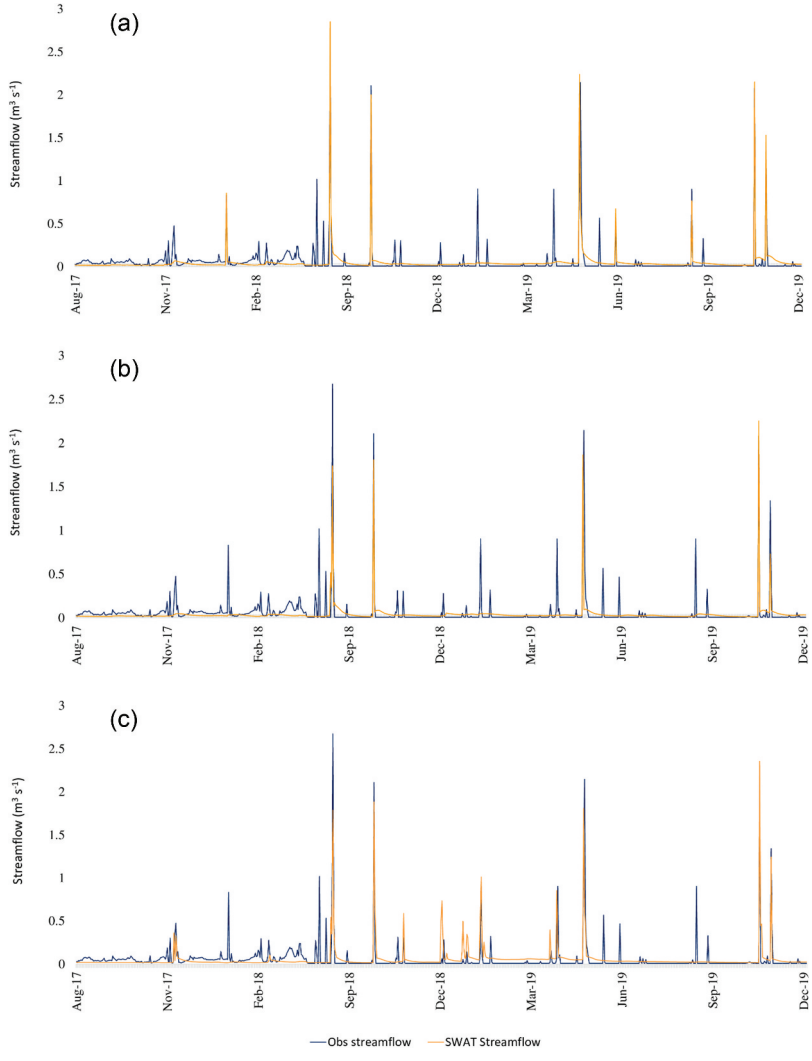

Figure 4. SWAT streamflow calibration of configurations A, B, and C at a daily time scale.

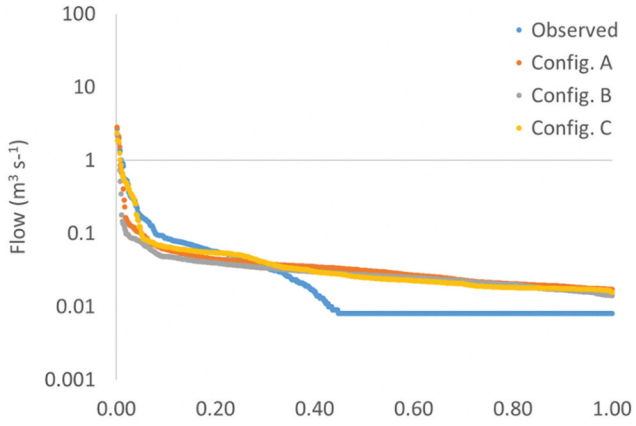

Figure 5. Flow duration curves of measured and simulated daily streamflow (2017–2019) at the outlet of the basin.

same percentage of rainfall even if the drainage area and the mean annual rainfall were different. Indeed, a huge difference was predicted in the percolation (water that percolates past the root zone, mm) between configuration C and configurations A and B, which showed a similar value (Table 4), indicating differences also in return flow. Differences were also predicted in the soil water content (mm) (Table 4).

4 Discussion

The application of hydrological models in Mediterranean basins may be particularly difficult because of the peculiarity of the flow regime, which is generally intermittent, and because of the presence of outcropping limestone and karst formations (Amin *et al.* 2017, Hartmann *et al.* 2021). In addition, the limited data availability that characterizes most of the small basins in the Mediterranean region may complicate model implementation and calibration (De Girolamo *et al.* 2022b). In this context, it is important to accurately build the conceptual model, taking into account the final aims of the modelling application and data availability. Hydrological models are able to generate long time-series of streamflow, which are fundamental to support river basin management and eco-hydrological studies also in ungauged basins or areas characterized by data scarcity (Ogie *et al.* 2017). Several studies demonstrated that the SWAT model is able to predict hydrological processes in different geographical (Jakada and Chen 2020) and hydrological conditions (Ricci *et al.* 2018, Borrelli *et al.* 2021). The groundwater dynamics play a crucial role in karst basins. Several attempts were made to address this issue by coupling SWAT with another model, by modifying some algorithms, or through a specific calibration (Nikolaidis *et al.* 2013a, Nerantzaki *et al.* 2015, Malagò *et al.* 2016, Martínez-Salvador and Conesa-García 2020). However, although some of those attempts successfully predicted the streamflow, the adopted procedures are generally difficult to replicate in different contexts. For this reason, the present study investigated an easy approach based on different schematizations of the basin in the SWAT model considering the karst areas contributing and not contributing to the streamflow, respectively. An additional approach was carried out by adopting a different parameterization in the model calibration.

The statistical performances for the streamflow simulation showed acceptable results for all configurations, confirming that SWAT is able to generate reliable streamflow series in basins with karst lithology (Amin *et al.* 2017). The results obtained in this study are slightly better than those reported by Eini *et al.* (2020), especially considering that the calibration was performed at a daily time scale.

Based only on the statistical criteria, configuration A performs better in terms of daily streamflow than B and C. In configuration A, the areas recharging the deep limestone aquifer were considered to not be actively contributing to surface runoff, and therefore were cut off before the SWAT model basin delineation (D'Ambrosio *et al.* 2020).

The remaining area (222 km^2), characterized by a homogeneous sandy-clay layer, allowed the model to better parameterize the fraction of transmission losses from the main channel (TRNSRCH.bsn), which can only be adjusted at the

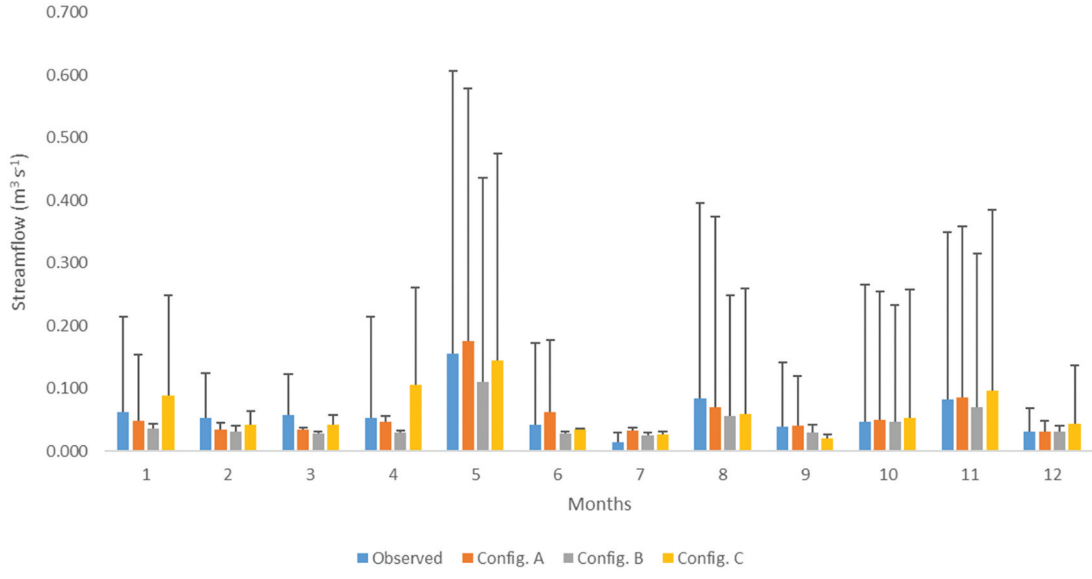

Figure 6. Observed and simulated mean monthly streamflow (m^2s^{-1}) for configurations A, B and C (2017–2019). Error bars represent the standard deviation.

Table 4. Mean annual components of the water balance estimated for configuration A (watershed delineation without karst areas), B (watershed delineation with karst areas), and C (watershed delineation with karst areas and calibrated with the crack flow function active) (2017–2019). Pcp: precipitation (mm); Eto: potential evapotranspiration (mm); Etr: actual evapotranspiration (mm); Surq: surface runoff (mm); Perc.: percolation (mm); SWC: soil water content (mm); TF: total flow (average annual flow out of the reach at the gauging station, mm); TWY: total water yield (total flow + deep aquifer – transmission losses, mm).

Configuration	Pcp	Eto	Etr	Surq	Perc	SWC	TF	TWY
A	621.44	1191.75	569.76	73.49	37.93	76.44	5.50	136.46
B	644.66	1161.64	575.97	51.62	43.57	60.83	4.30	96.17
C	644.66	1161.64	534.42	18.78	144.12	68.14	5.90	142.32

basin scale (Arnold *et al.* 2012a, 2012b). In contrast, when the whole drainage area (360 km^2) was considered for the basin delineation, as in configurations B and C, the average value assigned for the parameter TRNSRCH.bsn was not representative of the hydrological regime occurring in the upstream areas. In addition, the difference in drainage areas between configuration A and configurations B and C resulted in a diverse number of weather stations being considered by the model for the simulation. SWAT uses the centroid method to assign a weather station to the nearest sub-basin (Abdelwahab *et al.* 2018), hence external weather stations with respect to the basin area could be not included in the model set-up. In configuration A, only seven weather stations were effectively used by the model, while in configurations B and C nine stations were assigned to the sub-basin. This discrepancy resulted in different rainfall distributions and average annual precipitation and Eto value (Table 4). In areas characterized by a convective rainfall regime, such as the Mediterranean region, this aspect could be fundamental, since the number and the location of gauging stations directly influence the pattern of the rainfall and, consequently, the model uncertainty (Abdelwahab *et al.* 2018, Ehlers *et al.* 2019; Yen et al., 2018).

Going beyond the statistical performances and analysing the observed and the simulated streamflow (A, B, C) in the hydrographs and through the flow duration curves, it is evident that all the configurations overestimated the low flow periods. Several authors have already reported difficulties in modelling extremely low flow with the SWAT model due to uncertainty related to the parameterization of the multiple factors, (e.g. groundwater processes, topography, surface water exchanges with the subsoil, and management practices) (Guse *et al.* 2013, De Girolamo *et al.* 2017, 2022b, Ricci *et al.* 2018). Moreover, a certain degree of uncertainty related to WWTP input data may have contributed to the overestimation of the extremely low flow. Indeed, WWTP discharges are variable on the daily time scale, but due to the lack of data, constant annual values were used in this study to set up the model (D'Ambrosio *et al.* 2020). Configuration A better predicted extreme high flows and configuration C better estimated high and normal flows while configuration B underestimated all hydrological phases.

In the three configurations, the parameters such as the curve number (CN2), the deep aquifer percolation fraction (RCHRG_DP), the baseflow recession constant factor (ALPHA_BF), the groundwater revap coefficient (GW_REVAP), the hydraulic conductivity of the main channel (CH_K2), the Manning's roughness (CH_N2) of the main channel and the soil available water capacity for the first layer (SOL_AWC) proved to be very sensitive in the calibration process (Vale and Holman 2009, Martínez-Salvador and Conesa-García 2020). In particular, CN2 and CH_N2 were fundamental in improving the correspondence between observed and simulated peak flows and attenuating the flood waves in configurations A and B (Neitsch *et al.* 2011).

In configuration C, the activation of the crack flow function (SOL_CRK) permitted improving the simulation of the hydrological behaviour of the basin with respect to configuration B. SOL_CRK, which was originally introduced to replicate the crack development typical of Vertisols and to better simulate the flow bypassing the soil surface layer (Arnold *et al.* 2005), has already been used to represent the rapid flow processes in the soil profiles of karst-dominated catchments (Jarvis *et al.* 2016, Kan *et al.* 2019). Indeed, the high value of SOL_CRK used in the upstream sub-basins induced a higher percolation in soils (Table 4) and, consequently, allowed us to decrease the value of CH_N2. For this reason, in configuration C, the hydrograph showed also intermediate peaks which are not visible in configurations A and B (Fig. 4(c)). Hence, the crack flow function proved to be a valid option to improve the simulation of the hydrological processes occurring in karst areas.

Concerning the water balance components on a yearly basis, the results of the present work showed some differences between the configurations. In all the configurations most of the surface runoff was lost due to high transmission losses. Configuration B exhibited a value of TWY (96.17 mm) lower than those of A (136.46 mm) and C (142.32 mm), corresponding to 15% of precipitation (Table 4); meanwhile, the Etr was higher than that of A and C. This result can be explained by the fact that the automatic procedure adopted for the calibration (SWAT-CUP) forced the parameters related to the evapotranspiration (e.g. BIOMIX; CANMX) and groundwater (e.g. RCHRG_DP.gw, GW_REVAP.gw) in order to obtain the best fit of streamflow, which is a small component of the water balance due to the presence of the karst areas. Configuration C exhibited values of Surq and Etr lower than those of A and B; meanwhile, TWY for C was higher than that of A and B, indicating a higher groundwater recharge. TWY was 22% of precipitation in configurations A and C, showing that both approaches are good enough to predict water balance and streamflow in a Mediterranean environment.

In summarizing, differences between the configurations are due to both the spatial schematization and the model parameterization; the latter is recognized as a difficult phase that could influence the reliability of the results (Evenson *et al.* 2021, Ricci *et al.* 2022b). It is well known that manual calibration is time-consuming and that the automatic calibration

procedure carried out using the SWAT CUP or similar tools is very fast in identifying the best fit of parameters. However, the calibration of parameters using these tools requires particular caution. Indeed, the phenomenon of the "equifinality for different parameters" (different combinations of calibrated values providing similar model results) could lead to good statistical performances but an incorrect simulation of some physical and hydrological processes (Abbaspour 2015, Sánchez-Gómez *et al.* 2022). This issue can be partially solved by fixing an initial range of parameters based on the users' knowledge of the processes occurring in the basins (Arnold *et al.* 2015). However, additional information about Etr and groundwater recharge, if available, may contribute to improving the calibration and selecting the best modelling approach. Despite the above-mentioned differences, the three configurations well predicted the measured average total flow (5.8 mm), with a slight underestimation (5.5 mm and 4.3 mm, for A and B, respectively) or slight overestimation (5.9 mm for C) (Table 4).

The present study highlighted that a large uncertainty may be associated with the results of the model and that the final aim of the study (e.g. quantification of floods or low flow) should be taken into account in selecting the most appropriate approach as well as data availability and basin characteristics (i.e. karst area at the boundary or in the middle) (Abdelwahab *et al.* 2018, Jakada and Chen 2020).

5 Conclusions

Modelling daily streamflow in a Mediterranean environment with karst areas and an intermittent river network is generally a difficult task. The high spatial gradient in rainfall, the flow intermittency, and the limited data availability that characterize Mediterranean basins make modelling hydrological processes challenging. In this work, through a case study, three approaches based on a diverse basin delineation and on different model parameterizations were tested to predict daily streamflow using the SWAT model.

The results show that the SWAT model was able to simulate daily streamflow in a Mediterranean environment with karst areas. The model performances were satisfactory for configurations B and C and good for A. However, all the approaches overestimated the low flow, confirming several studies carried out in the Mediterranean region. Configuration A showed the best performance in simulating large floods, and configuration C presented the best fit of monthly low flow, from May to July. Differences in water balance components were detected among the three configurations: C showed a lower surface runoff, lower values of TWY and higher deep aquifer recharge than A and B. At the basin scale, TWY was 22% of precipitation for both A and C.

Several factors, such as the final aim of the study, data availability, and the characteristics of the basin should be considered in selecting the best model configuration. However, some limitations of the approaches presented in this study can be pointed out. The cut-off of the karst areas (configuration A) is a valid option only if the karst formations are localized at the edges of the basin and if these areas do not contribute to the streamflow. This aspect needs to be verified with field surveys in order to ascertain the absence of flow in the river network within these areas (i.e. monitoring or field surveys). The Crack Flow function (configuration C), instead, can be adopted by the user if there are karst areas inside the basin that cannot be cut off, but it requires a knowledge of the area and an accurate spatial distribution of the karst formation to identify the sub-basins where the Crack Flow function has to be activated. Finally, configuration B represents an easy approach that does not require specific experience in modelling and it is suggested to be adopted when lithological data are poor but a large uncertainty may affect the results.

Further studies and field measurements are needed to improve the predictions of water balance components such as evapotranspiration and groundwater recharge.

CRediT authorship contribution statement Giovanni Francesco Ricci: conceptualization, methodology, writing – original draft, writing – review and editing, investigation, data curation. **Marco Centanni**: methodology, visualization, investigation, data curation, writing – original draft. **Anna Maria De Girolamo**: conceptualization, supervision, validation, methodology, writing – original draft, writing – review and editing, visualization. **Francesco Gentile**: conceptualization, supervision, writing – review and editing, project administration.

Acknowledgements

The authors of the paper thank the reviewers and the editors for their useful comments and recommendations that helped to improve the manuscript.

Disclosure statement

No potential conflict of interest was reported by the authors.

Funding

This work was supported by the Italian Ministry of University and Research (MIUR), and the Program "Partnership for Research and Innovation in the Mediterranean Area" (PRIMA 2018), Project INWAT "Quality and management of intermittent river and groundwater in the Mediterranean basins."

ORCID

Giovanni Francesco Ricci http://orcid.org/0000-0001-6724-8789
Marco Centanni http://orcid.org/0000-0003-2983-145X
Anna Maria DeGirolamo http://orcid.org/0000-0001-5605-6239
Francesco Gentile http://orcid.org/0000-0003-4462-0466

References

Abbaspour, K.C., 2015. *Calibration and uncertainty programs for SWAT. SWAT-CUP: SWAT calibration and uncertainty programs – a user manual.* Dübendorf, Switzerland: Eawag.

Abdelwahab, O.M.M., *et al.*, Oct 2018. Modelling soil erosion in a Mediterranean watershed: comparison between SWAT and AnnAGNPS models. *Environmental Research*, 166, 363–376. doi:10.1016/j.envres.2018.06.029

Acuña, V., *et al.*, 2014. Why should we care about temporary waterways? *Science*, 343 (6175), 1080–1081. doi:10.1126/science.1246666

Amin, M.G.M., *et al.*, 2017. Simulating hydrological and nonpoint source pollution processes in a karst watershed: a variable source area hydrology model evaluation. *Agricultural Water Management*, 180, 212–223. doi:10.1016/j.agwat.2016.07.011

Arnold, J.G., *et al.*, 2012a. SWAT: model use, calibration, and validation. *Transactions of the ASABE*, 55 (4), 1491–1508. doi:10.13031/2013.42256

Arnold, J.G., *et al.*, 2012b. *Soil & Water Assessment Tool: Input/Output Documentation Version 2012*. Texas Water Resource Institute.

Arnold, J.G., *et al.*, 2005. Estimation of soil cracking and the effect on surface runoff in a Texas Blackland Prairie watershed. *Hydrological Processes*, 19 (3), 589–603. doi:10.1002/hyp.5609

Arnold, J.G., *et al.*, 1998. Large area hydrologic modeling and assessment – part 1: model development. *Journal of the American Water Resources Association*, 34 (1), 73–89. doi:10.1111/j.1752-1688.1998.tb05961.x

Arnold, J.G., *et al.*, 2015. Hydrological processes and model representation: impact of soft data on calibration. *Transactions of the ASABE*, 58 (6), 1637–1660.

Arsenault, R., Brissette, F., and Martel, J.L., 2018. The hazards of split-sample validation in hydrological model calibration. *Journal of Hydrology*, 566 (September), 346–362. doi:10.1016/j.jhydrol.2018.09.027

Baffaut, C. and Benson, V.W., 2009. Modeling flow and pollutant transport in a Karst Watershed with SWAT. *Transactions of the ASABE*, 52 (2), 469–479. doi:10.13031/2013.26840

Borg Galea, A., *et al.*, 2019. Mediterranean intermittent rivers and ephemeral streams: challenges in monitoring complexity. *Ecohydrology*, 12 (8), 1–11. doi:10.1002/eco.2149

Borrelli, P., *et al.*, 2021. Soil erosion modelling: a global review and statistical analysis. *Science of the Total Environment*, 780, 146494. doi:10.1016/j.scitotenv.2021.146494

Borrelli, P., *et al.*, 2016. Effect of good agricultural and environmental conditions on erosion and soil organic carbon balance: a national case study. *Land Use Policy*, 50, 408–421. doi:10.1016/j.landusepol.2015.09.033

D'Ambrosio, E., *et al.*, 2017. Characterising the hydrological regime of an ungauged temporary river system: a case study. *Environmental Science and Pollution Research*, 24 (16), 13950–13966. doi:10.1007/s11356-016-7169-0

D'Ambrosio, E., *et al.*, 2019. A spatial analysis to define data requirements for hydrological and water quality models in data-limited regions. *Water*, 11 (2), 267. doi:10.3390/w11020267

D'Ambrosio, E., *et al.*, 15 Dec 2020. Using water footprint concepts for water security assessment of a basin under anthropogenic pressures. *Science of the Total Environment*, 748, 141356. doi:10.1016/j.scitotenv.2020.141356

Datry, T., Bonada, N., and Boulton, A.J., 2017. Chapter 1 - general introduction. Intermittent rivers and ephemeral streams. *Ecology and Management*, 2017, 1–20. doi:10.1016/B978-0-12-803835-2.00001-2

De Filippis, G., *et al.*, 2017. Effects of different boundary conditions on the simulation of groundwater flow in a multi-layered coastal aquifer system (Taranto Gulf, southern Italy). *Hydrogeology Journal*, 25, 2123–2138. doi:10.1007/s10040-017-1589-x

De Girolamo, A., *et al.*, 2017. Simulating ecologically relevant hydrological indicators in a temporary river system. *Agricultural Water Management*, 180 (Part B), 194–204. doi:10.1016/j.agwat.2016.05.034

De Girolamo, A.M., *et al.*, 2022a. Modelling effects of forest fire and post-fire management in a catchment prone to erosion: impacts on sediment yield. *Catena*, 212, 106080. doi:10.1016/j.catena.2022.106080

De Girolamo, A.M., *et al.*, 2022b. Characterising flow regimes in a semi-arid region with limited data availability: the Nil Wadi case study (Algeria). *Journal of Hydrology: Regional Studies*, 41 (November 2021), 101062. doi:10.1016/j.ejrh.2022.101062

De Girolamo, A.M., *et al.*, 20 Dec 2019. Developing a nitrogen load apportionment tool: theory and application. *Agricultural Water Management*, 226, 105806. doi:10.1016/j.agwat.2019.105806

EC, 2000. EU Water Framework Directive.

EC, 2019. 640, Communication from the commission to the European parliament, the European council, the council, the European economic and social committee and the committee of the regions. Eur. Green Deal.

Ehlers, L.B., Sonnenborg, T.O., and Refsgaard, J.C., 2019. Observational and predictive uncertainties for multiple variables in a spatially distributed hydrological model. *Hydrological Processes*, 33 (5), 833–848.

Eini, M.R., *et al.*, 2020. Development of alternative SWAT-based models for simulating water budget components and streamflow for a karstic-influenced watershed. *Catena*, 195 (July), 104801. doi:10.1016/j.catena.2020.104801

Evenson, G.R., *et al.*, 2021. Uncertainty in critical source area predictions from watershed-scale hydrologic models. *Journal of Environmental Management*, 279, 111506. doi:10.1016/j.jenvman.2020.111506

Fortesa, J., *et al.*, 2021. Analysing hydrological and sediment transport regime in two Mediterranean intermittent rivers. *Catena*, 196 (September 2020), 104865. doi:10.1016/j.catena.2020.104865

Fovet, O., *et al.*, 2021. Intermittent rivers and ephemeral streams: perspectives for critical zone science and research on socio-ecosystems. *Wiley Interdisciplinary Reviews: Water*, 8 (4), 1–33. doi:10.1002/wat2.1523

Green, W.H. and Ampt, G., 1911. Studies on soil physics, 1. The flow of air and water through soils. *The Journal of Agricultural Science*, 4, 11–24.

Guse, B., Reusser, D.E., and Fohrer, N., 2013. How to improve the representation of hydrological processes in SWAT for a lowland catchment—temporal analysis of parameter sensitivity and model performance. *Hydrological Processes*. doi:10.1002/hyp.9777

Hargreaves, H.G.A. and Samani, Z., 1985. Reference crop evapotranspiration from temperature. *Applied Engineering in Agriculture*, 1 (1985), 96. doi:10.13031/2013.26773

Hartmann, A., *et al.*, 2021. Integrating field work and large-scale modeling to improve assessment of karst water resources. *Hydrogeology Journal*, 29, 315–329. doi:10.1007/s10040-020-02258-z

Jakada, H. and Chen, Z., 2020. An approach to runoff modelling in small karst watersheds using the SWAT model. *Arabian Journal of Geosciences*, 13 (8). doi:10.1007/s12517-020-05291-0

Jarvis, N., Koestel, J., and Larsbo, M., 2016. Understanding preferential flow in the vadose zone: recent advances and future prospects. *Vadose Zone Journal*, 15 (12), vzj2016.09.0075. doi:10.2136/vzj2016.09.0075

Jimeno-Sáez, P., *et al.*, 2018. A comparison of SWAT and ANN models for daily runoff simulation in different climatic zones of Peninsular Spain. *Water*, 10, 192. 10.3390/w10020192

Kan, X., *et al.*, 2019. Effects of grass and forests and the infiltration amount on preferential flow in karst regions of China. *Water*, 11 (8), 1–19. doi:10.3390/w11081634

Lisco, S., *et al.*, 2016. Geology of Mar Piccolo, Taranto (southern Italy): the physical basis for remediation of a polluted marine area. *Journal of Maps*, 12 (1), 173–180. doi:10.1080/17445647.2014.999136

Malagò, A., *et al.*, 2016. Regional scale hydrologic modeling of a karst-dominant geomorphology: the case study of the Island of Crete. *Journal of Hydrology*, 540, 64–81. doi:10.1016/j.jhydrol.2016.05.061

Martínez-Salvador, A. and Conesa-García, C., 2020. Suitability of the SWAT model for simulating water discharge and sediment load in a Karst Watershed of the Semiarid mediterranean basin. *Water Resources Management*, 34 (2), 785–802. doi:10.1007/s11269-019-02477-4

Meresa, H., 2019. Modelling of river flow in ungauged catchment using remote sensing data: application of the empirical (SCS-CN), artificial neural network (ANN) and hydrological model (HEC-HMS). *MESE*, 5, 257–273. doi:10.1007/s40808-018-0532-z

Monteith, J., 1965. Evapotranspiration and the environment. The state and movement of water in living organisma. In: *Proceedings of the XIXth Symposium Society for Experimental Biology*. Swansea: Cambridge University Press.

Moriasi, D.N., *et al.*, 2007. Model evaluation guidelines for systematic quantification of accuracy in watershed simulations. *Transactions of the ASABE*, 50 (3), 885–900. doi:10.13031/2013.23153

Nash, J.E. and Sutcliffe, J.V., 1970. River flow forecasting through conceptual models part I – a discussion of principles. *J. Hydrol*, 1010 (70), 282–290.

Neitsch, S.L., *et al.*, 2011. Soil and water assessment tool: theoretical documentation V. 2009 Texas Water Resources Institute Technical Report No. 406. Texas: Texas A&M University System College Station.

Nerantzaki, S.D., *et al.*, 2015. Modeling suspended sediment transport and assessing the impacts of climate change in a karstic Mediterranean watershed. *Science of the Total Environment*, 538, 288–297. doi:10.1016/j.scitotenv.2015.07.092

Nikolaidis, N.P., Bouraoui, F., and Bidoglio, G., 2013a. Hydrologic and geochemical modeling of a karstic Mediterranean watershed. *Journal of Hydrology*, 477, 129–138. doi:10.1016/j.jhydrol.2012.11.018

Nikolaidis, N.P., *et al.*, 2013b. Towards a sustainable management of Mediterranean river basins. Policy recommendations on management aspects of temporary river basins. *Water Policy*, 15, 830–849. doi:10.2166/wp.2013.158

Ogie, R.I., *et al.*, 2017. Optimal placement of water-level sensors to facilitate data-driven management of hydrological infrastructure assets in coastal mega-cities of developing nations. *Sustainable Cities and Society*, 35, 385–395. doi:10.1016/j.scs.2017.08.019

Oueslati, O., *et al.*, 2015. Classifying the flow regimes of Mediterranean streams using multivariate analysis. *Hydrological Processes*, 29 (22), 4666–4682. doi:10.1002/hyp.10530

Poff, N.L.R., *et al.*, 1997. The natural flow regime: a paradigm for river conservation and restoration. *BioScience*, 47 (11), 769–784. doi:10.2307/1313099

Polemio, M., Dragone, V., and Limoni, P.P., 2008. Salt contamination of Apulian aquifers: spatial and time trend. 19th SWIM & 3rd SWICA jointed meeting: Cagliari, 115–121.

Priestley, C.H.B. and Taylor, R.J., 1972. On the assessment of surface heat flux and evaporation using large-scale parameters. *Monthly Weather Review*, 100 (1972), 81–92. doi:10.1175/1520-0493(1972)100<0081:OTAOSH>2.3.CO;2

Ricci, G.F., *et al.*, 2018. Identifying sediment source areas in a Mediterranean watershed using the SWAT model. *Land Degradation and Development*, 29 (4), 1233–1248. doi:10.1002/ldr.2889

Ricci, G.F., *et al.*, 2020. Effectiveness and feasibility of different management practices to reduce soil erosion in an agricultural watershed. *Land Use Policy*, 90, 104306. doi:10.1016/j.landusepol.2019.104306

Ricci, G.F., *et al.*, 2022a. Evaluating flow regime alterations due to point sources in intermittent rivers: a modelling approach. *Journal Of Agricultural Engineering*, 53. doi:10.4081/jae.2022.1333

Ricci, G.F., *et al.*, 2022b. Efficiency and feasibility of best management practices to reduce nutrient loads in an agricultural river basin. *Agricultural Water Management*, 259 (May 2021), 107241. doi:10.1016/j.agwat.2021.107241

Sánchez-Gómez, A., *et al.*, 2022. Optimization of a SWAT model by incorporating geological information through calibration strategies. *Optimization and Engineering*, 23 (4), 2203–2233. doi:10.1007/s11081-022-09744-1

Sauquet, E., *et al.*, 2021. Classification and trends in intermittent river flow regimes in Australia, northWestern Europe and USA: a global perspective. *Journal of Hydrology*, 597, 126170. doi:10.1016/j.jhydrol.2021.126170

Senent-Aparicio, J., *et al.*, 2020. Coupling SWAT model and CMB method for modeling of high-permeability Bedrock basins receiving interbasin groundwater flow. *Water*, 12, 657. doi:10.3390/w12030657

Soria, M., *et al.*, 2021. Adapting participatory processes in temporary rivers management. *Environmental Science & Policy*, 120, 145–156. doi:10.1016/j.envsci.2021.03.005

Tramblay, Y., *et al.*, 2020. Trends in flow intermittence for European rivers. *Hydrological Sciences Journal*, 66 (1), 37–49. doi:10.1080/02626667.2020.1849708

Vale, M. and Holman, I.P., 2009. Understanding the hydrological functioning of a shallow lake system within a coastal karstic aquifer in Wales, UK. *Journal of Hydrology*, 376 (1–2), 285–294. doi:10.1016/j.jhydrol.2009.07.041

van Meerveld, H.J.I., *et al.*, 2020. Aqua temporaria incognita. *Hydrological Processes*, 34 (26), 5704–5711. doi:10.1002/hyp.13979

Winchell, M., *et al.*, 2013. ArcSWAT interface for SWAT2012 user's guide blackland research and extension center, temple. TXTR 439–464.

Yen, H., *et al.*, 15 Oct 2018. Input uncertainty on watershed modeling: evaluation of precipitation and air temperature data by latent variables using SWAT. *Ecological Engineering*, 122, 16–26. doi:10.1016/j.ecoleng.2018.07.014

Zuffianò, L.E., *et al.*, 2016. Coastal hydrogeological system of Mar Piccolo (Taranto, Italy). *Environmental Science and Pollution Research*, 23, 12502–12514. doi:10.1007/s11356-015-4932-6